HIGH-RESOLUTION ULTRASOUND VISUALIZATION OF THE DEEP BRANCH OF THE ULNAR NERVE

GEORG RIEGLER, MD,[1] DORIS LIEBA-SAMAL, MD,[2] PETER C. BRUGGER, MD, PhD,[3] CHRISTOPHER PIVEC, MD,[1] HANNES PLATZGUMMER, MD,[1] MARTIN VIERHAPPER, MD,[4] GABRIELA MUSCHITZ, MD, PhD,[4] SUREN JENGOJAN, MD,[1] and GERD BODNER, MD[1]

[1] Department of Biomedical Imaging and Image-Guided Therapy, Medical University of Vienna, Währingergürtel 18-20, 1090 Vienna, Austria
[2] Department of Neurology, Medical University of Vienna, Vienna, Austria
[3] Department of Anatomy, Center for Anatomy and Cell Biology, Medical University of Vienna, Vienna, Austria
[4] Department of Surgery, Medical University of Vienna, Vienna, Austria

Accepted 14 February 2017

ABSTRACT: *Introduction*: The value of imaging the deep branch of the ulnar nerve (DBUN) over its entire course has not been clarified. Therefore, this study evaluates the feasibility of visualizing the DBUN from its origin to the most distal point. *Methods*: We performed high-resolution ultrasound (HRUS) with high-frequency probes (18–22 MHZ), HRUS-guided ink marking, and consecutive dissection in 8 fresh cadaver hands. In both hands of 10 healthy volunteers (n = 20), the cross-sectional area (CSA) was measured at 2 different locations (R1 and R2). *Results*: The DBUN was clearly visible in all anatomical specimens and in healthy volunteers. Dissection confirmed HRUS findings in all anatomical specimens. The mean CSA was 1.8 ± 0.5 mm^2 at R1 and 1.6 ± 0.4 mm^2 at R2. *Discussion*: This study confirms that the DBUN can be reliably visualized over its entire course with HRUS in anatomical specimens and in healthy volunteers.

Muscle Nerve **56**: 1101–1107, 2017

The deep branch of the ulnar nerve (DBUN) is a terminal motor branch that usually divides from the ulnar nerve within or just proximal to the Guyon canal.[1,2] It then follows the medial wall of the hook of the hamate bone beneath the pisohamate ligament and continues on a distal and lateral course to pass the hypothenar musculature.[2] The DBUN follows the course of the deep palmar arch beneath the flexor tendons and ends by innervating the adductor pollicis and flexor pollicis brevis muscles (Fig. 1). Other muscles innervated by the DBUN are the opponens digiti minimi, abductor digiti minimi, flexor digiti minimi brevis, interossei, and lumbricals to the ring and small fingers.[1]

The classical isolated lesion of the DBUN is clinically known as type II Guyon canal syndrome.[3] Lesions of the branch distal to the Guyon canal[4] are less commonly diagnosed or potentially underrecognized because of a lack of evaluation tools that can depict the whole nerve. The clinical presentation of DBUN neuropathy can include loss of finger coordination, cramping, and weakness in grip and pinch strength. The worst cases present with hypothenar atrophy and clawing of the fourth and fifth fingers.[3,5]

Various reasons for DBUN-related lesions have been described. Ganglion cysts,[4–7] repetitive trauma caused by prolonged pressure (e.g., bicycling)[8,9] or vibratory tools (e.g., jackhammers),[10] and anatomical variations[11,12] are frequently described pathologies. Other, more rare, etiologies include tumors,[13,14] fractures,[15] iatrogenic injury,[16] arthritis-associated complications,[6] and coexisting carpal tunnel syndrome.[17] Moreover, the DBUN risks compression as it passes beneath the pisohamate ligament[18] or the arch of the adductor pollicis muscle.[19]

In addition to clinical assessment, electrodiagnostic testing may help evaluate DBUN lesions.[20] However, electromyography is painful and invasive and cannot characterize the secondary causes. MRI and ultrasound have been proposed as feasible methods with which to demonstrate etiologies related to the DBUN within the Guyon canal.[12,21] Currently, however, no study has clarified the actual value of imaging the DBUN to its most distal point.

Because high-resolution ultrasound (HRUS) offers excellent tissue differentiation for examination of superficial structures, we hypothesize that DBUN evaluation is possible over the entire course of the nerve. This could allow for precise assessment of DBUN lesions and subsequently improve targeted therapy.

This study, therefore, seeks first to confirm the correct identification of the DBUN by HRUS with ink marking and consecutive dissection in anatomical specimens and second to provide initial measurements of DBUN diameter in healthy volunteers.

MATERIALS AND METHODS

Ultrasound Examination Technique. This prospective study was conducted between February 1, 2015, and July 1,

Abbreviations: CSA, cross-sectional area; DBUN, deep branch of the ulnar nerve; HRUS, high-resolution ultrasound; LD, transverse long axis diameter; SD, transverse short axis diameter

Key words: ganglion cysts; iatrogenic disease; ulnar nerve; ulnar nerve compression syndrome; ultrasonography

Conflicts of Interest: None of the authors have any conflict of interest to disclose.

Correspondence to: G. Riegler;

© 2017 Wiley Periodicals, Inc.

Published online 18 February 2017 in Wiley Online Library (wileyonlinelibrary.com). DOI 10.1002/mus.25614

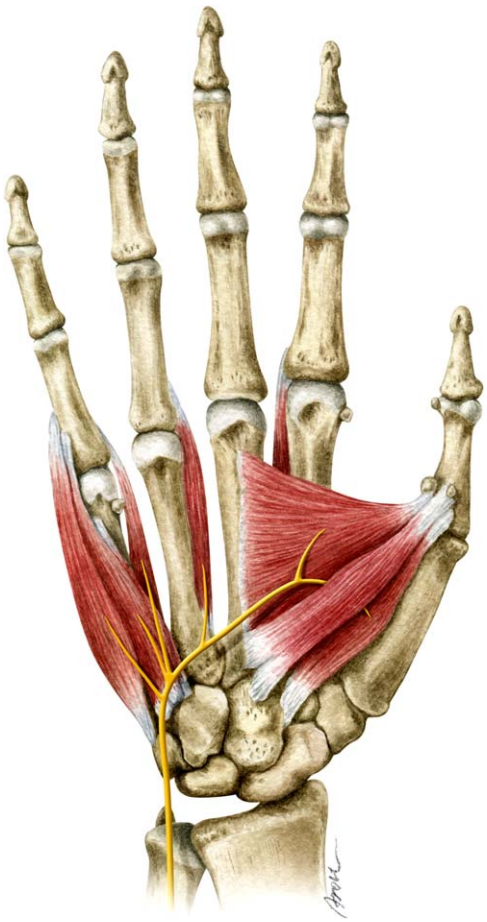


FIGURE 1. Illustration of the course of the DBUN. To better visualize the DBUN, the third and fourth lumbrical muscles and the dorsal interosseous muscles, which are also innervated by the DBUN, were removed.

2015. It was approved by the local ethics committee of the Medical University of Vienna (EC-No. 1529/2015). HRUS examinations were carried out with a GE LOGIQ e (GE Healthcare, Wauwatosa, WI) ultrasound platform with high-frequency probes (GE L8-18i-D, GE L10-22-RS). Both ultrasound probes have wide-band high frequencies (ranging from 8 to 22 MHZ) to allow for ultrasound assessment of superficial structures. The GE L10-22-RS probe, compared with the L8-18i-D, comes with the advantage of even higher frequencies, which allows for delineation of very small (sub-millimeter) superficial structures, but with the disadvantage of very limited tissue penetration (approximately 2 cm). Two radiologists carried out all examinations. One had more than 20 years experience (G.B.) and one had 4 years experience (G.R.) in peripheral nerve imaging. Both raters were present during the recruitment of the individuals. G.B. performed all interventions on all anatomical specimens. G.R. collected all images of healthy individuals and observed the procedure.

The evaluation followed a standardized assessment protocol, starting with a transverse view of the ulnar nerve approximately 3 cm proximal to the pisiform bone. The nerve was then tracked distally toward the palm until it divided into superficially and deeply located branches. The deeply located branch was presumed to be the DBUN. The relation of the bifurcation of the ulnar nerve to the pisiform bone (proximal, distal, or at the level of the pisiform) was noted. After identification, the nerve was followed distally, passing medially to the hook of the hamate and deeply coursing toward the thenar until its entrance into the adductor pollicis brevis muscle. To obtain a better overview of the scanned region, the examination always started with the GE L8-18i-D probe. After identification and initial assessment of the DBUN, the transducer was changed to an L10-22-RS probe to better delineate the echotexture of the DBUN. At the superficial location of the DBUN (proximal to the hook of the hamate), the image depth was adjusted to a maximum of 1 cm, whereas, at its course through the deep palm, the depth of the image required constant adjustment from 1 cm to a maximum of 2 cm (depending on the fatty tissue that overlies this region). Because of the course of the DBUN, special attention was required to angulate the probe to avoid anisotropy and to ensure that the nerve was in full view and not distorted in the image. The whole nerve was assessed by using transverse and longitudinal views. Color Doppler was used in healthy volunteers to avoid confusion with the deep palmar artery. Examinations were documented with both still images and dynamic video sequences. Probe positioning and normal presentation of the DBUN is shown in Figure 2.

Ultrasound in Anatomical Specimens. In 4 randomly selected fresh anatomical specimens in the legal custody of the Department of Anatomy, Medical University of Vienna, HRUS was performed as described above in both hands (n = 8). After localizing the DBUN, a small amount of blue dye mixed with glue (0.1 ml) was injected into the nerve or adjacent to it under HRUS guidance (22-gauge needle, in-plane technique) shortly after its separation from the ulnar nerve and next to its entrance into the adductor pollicis muscle between the third and fourth metacarpal bones. Subsequent anatomical dissection was performed to confirm the exact location of the dye injection.

Ultrasound in Healthy Volunteers. Ten healthy volunteers were recruited via a notice displayed at the Department of Biomedical Imaging and Image-Guided Therapy and by word of mouth. Written informed consent was obtained from all volunteers. Inclusion criteria were age >18 years and ability to give written, informed consent. Exclusion criteria were known polyneuropathy, known myopathy, chronic disease known to cause peripheral neuropathy, current or previous Guyon's canal syndrome, and previous hand surgery. The DBUN was assessed on both sides (n = 20).

The transverse long axis diameter (LD), the transverse short axis diameter (SD), and the cross-sectional area (CSA) were measured at 2 locations, directly after the separation from the ulnar nerve (R1) and atop the fourth metacarpal bone (R2), with the LOGIQ e platform software. The measurements were calculated with the probe perpendicular to the main nerve course in the transverse plane with adequate magnification and zoom.

Statistical Analysis. Descriptive statistics were performed in SPSS Statistics for Windows version 22.0.0.2 (IBM, Armonk, New York). Metric data (nerve diameter) are presented as mean ± standard deviation and range (minimum to maximum).

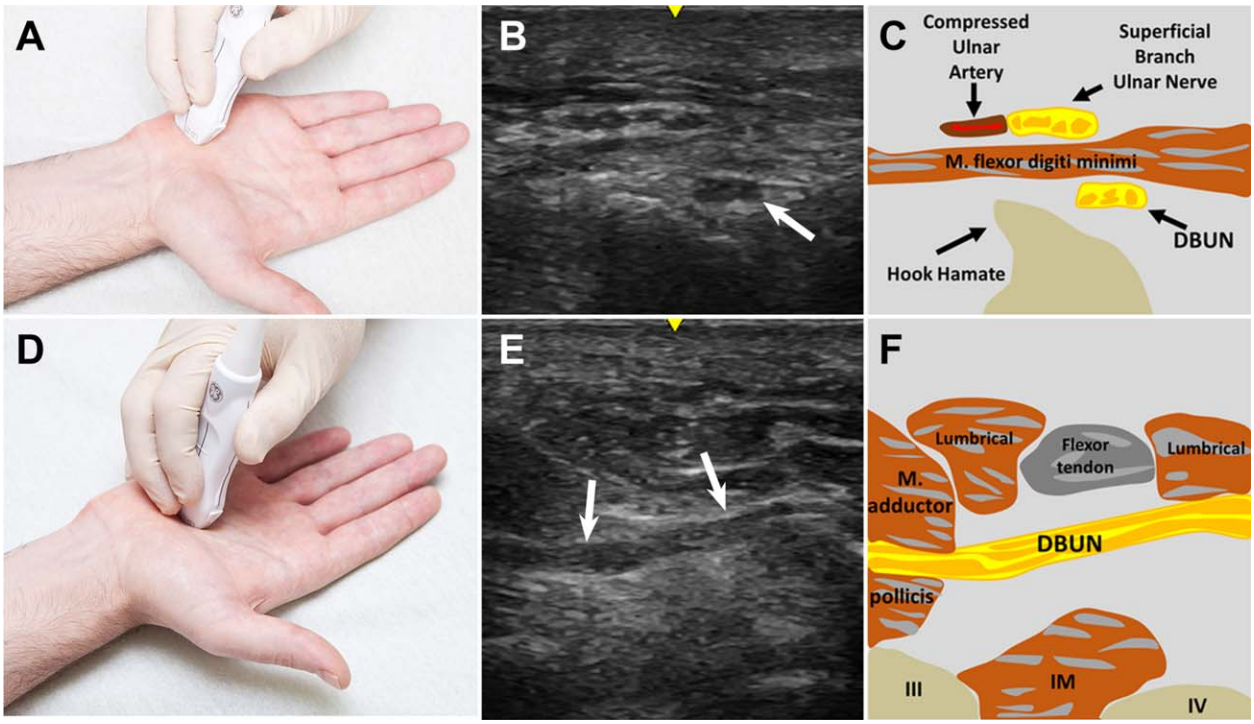


FIGURE 2. An example of probe positioning (**A**), sonographic findings of the DBUN (marked with arrows; **B**), and graphical illustrations of the nerve, approximately 1 cm distal to its subdivision from the ulnar nerve (**C**). (**D,E**) Longitudinal view of the branch entering the deep palm and the adductor pollicis muscle. (**F**) Graphical illustration of the nerve.

RESULTS

Ultrasound in Anatomical Specimens. The DBUN was clearly visible in all anatomical specimens. Dissection confirmed the correct identification of the DBUN (100%) on both sides in all subjects (n = 8). An example of a dissection finding is shown in Figure 3. The ulnar nerve bifurcation in anatomical specimens was proximal to the pisiform bone in 3 specimens, at the pisiform bone in 4 specimens, and distal to the pisiform bone in 1 specimen.

Ultrasound in Healthy Volunteers. Table 1 summarizes the demographic findings and measurements. Five women and 5 men (mean age, 31.5 years; age range, 27–54 years) were included in the study. In all volunteers, the DBUN could be visualized in both wrists (n = 20). Assessment of the nerve was possible from its origin to its entrance into the adductor pollicis muscle. The normal appearance of the DBUN was of a honeycombed structure with fascicles and a small, surrounding, slightly hyperechoic border. The nerve had a circular/ovoid shape over its entire course.

The mean LD in volunteers was 1.6 ± 0.3 mm (range, 0.9–2.0 mm) at R1 and 1.5 ± 0.2 mm (range, 1.1–1.8 mm) at R2. The mean SD in volunteers was 1.2 ± 0.2 mm (range, 0.8–1.7 mm) at R1 and 1.1 ± 0.2 mm (range, 0.8–1.4 mm) at R2.

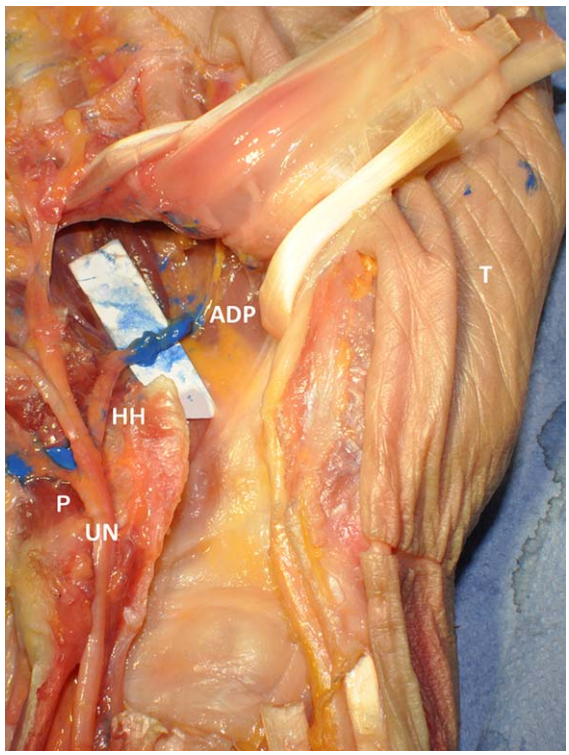


FIGURE 3. Example of dissection findings after HRUS-guided intranerve ink marking of the DBUN next to its entrance to the adductor pollicis brevis muscle. ADP, adductor pollicis muscle; HH, hook of the hamate; P, pisiform bone; T, thenar; UN, ulnar nerve.

Table 1. Demographic characteristics and measurements of the DBUN in healthy volunteers.

Volunteer	Sex	Age (y)	Side	LD1 (mm)	SD1 (mm)	CSA1 (mm^2)	LD2 (mm)	SD2 (mm)	CSA2 (mm^2)
1	M	31	R	1.8	1.3	1.9	1.5	1.4	2.0
1	M	31	L	1.7	1.2	1.8	1.1	1.1	1.4
2	M	33	R	1.7	1.1	1.7	1.6	1.1	1.8
2	M	33	L	1.7	1.1	1.7	1.5	1.2	1.9
3	M	55	L	1.5	1.3	1.8	1.9	1.1	2.2
3	M	55	R	1.3	0.9	1.1	1.7	1.1	1.8
4	W	38	R	1.6	1.4	2.2	1.5	1.3	1.8
4	W	38	L	1.3	1.3	1.4	1.8	1.3	1.7
5	W	31	R	0.9	0.9	0.9	1.2	1.1	1.1
5	W	31	L	1.1	1.0	1.3	1.2	1.1	1.1
6	W	30	R	1.9	1.4	2.6	1.6	1.0	1.6
6	W	30	L	1.7	1.0	1.9	1.5	1.1	1.6
7	W	54	R	2.0	1.7	3.2	1.8	1.2	2.1
7	W	54	L	2.0	1.5	2.5	1.2	1.2	1.4
8	M	32	R	1.6	1.3	1.7	1.5	0.9	1.6
8	M	32	L	1.3	0.8	1.2	1.2	0.8	0.9
9	W	27	R	1.7	1.1	1.9	1.7	1.0	1.7
9	W	27	L	1.4	0.9	1.4	1.1	0.9	0.9
10	M	31	R	1.6	0.9	1.4	1.6	1.2	1.8
10	M	31	L	1.6	0.9	1.9	1.6	1.0	1.3
Mean				1.6	1.2	1.8	1.5	1.1	1.6
Standard deviation				0.3	0.2	0.6	0.2	0.2	0.4

CSA, cross-sectional area; DBUN, deep branch of the ulnar nerve; L, left; LD, long axis diameter; M, man; R, right; SD, short axis diameter; W, woman; y, years.

The maximum detectable side difference in LD was 0.3 mm at R1 and 0.6 mm at R2, and in SD it was 0.5 mm at R1 and 0.3 mm at R2. The mean CSA was 1.8 ± 0.5 mm^2 at R1 and 1.6 ± 0.4 mm^2 at R2. No aberrant branch of the DBUN was detected.

The ulnar nerve bifurcation in healthy volunteers was proximal to the pisiform bone in 6 individuals, at the pisiform bone in 11 individuals, and distal to the pisiform bone in 3 individuals. No aberrant branch of the DBUN was detected. Examples of ultrasound measurements are shown in Fig. 4).

DISCUSSION

The results of this study confirm that DBUN can be reliably visualized and evaluated over its entire course by HRUS with ultrasound-guided ink marking and consecutive dissection in a series of anatomical specimens. Furthermore, we present the measurements of the DBUN at 2 different locations in healthy volunteers, with a mean diameter of 1.6 ± 0.3 mm (range, 0.9–2.0 mm) at its proximal location and 1.5 ± 0.2 mm (range, 1.1–1.8 mm) at its distal location.

In some cases, the diagnosis of DBUN neuropathy may be challenging because of variable muscle involvement, depending on the site of damage. If damage occurs proximal to the branch to the hypothenar muscles, clinical and electrodiagnostic testing can, for the most part, be used to diagnose a DBUN neuropathy. If damage occurs further distally, the underlying pathology of DBUN neuropathies remains unclear[22] and cannot be determined without imaging methods or surgical exploration.

Using the assessment protocol proposed in this study, we can use HRUS to depict the nerve over its entire course. Although our results are based on healthy volunteers and additional studies are required to clarify the role of HRUS in patients, we think HRUS may play a crucial role in assessing patients with suspected DBUN neuropathies. This may allow more precise patient management. For example, in cases of idiopathic DBUN caused by excessive mechanical stress (such as prolonged pressure in cycling or using vibratory tools such as jackhammers), conservative treatment options, such as splinting, can be expected to be sufficient, whereas secondary DBUN neuropathies caused by space-occupying lesions require surgical treatment to reduce pressure on the nerve and avoid irreversible muscle atrophy caused by long-time denervation. Therefore, HRUS may help to identify lesions that require surgery.

In this way, unnecessary surgical exploration with its associated risk could be avoided, and, consequently, this may decrease patient discomfort and increase patient safety. Finally, ultrasound-guided therapeutic options, such as ganglion cyst aspiration and needling[23] or botulinum toxin injections in cases of anomalous muscles, may be therapeutic options.[24]

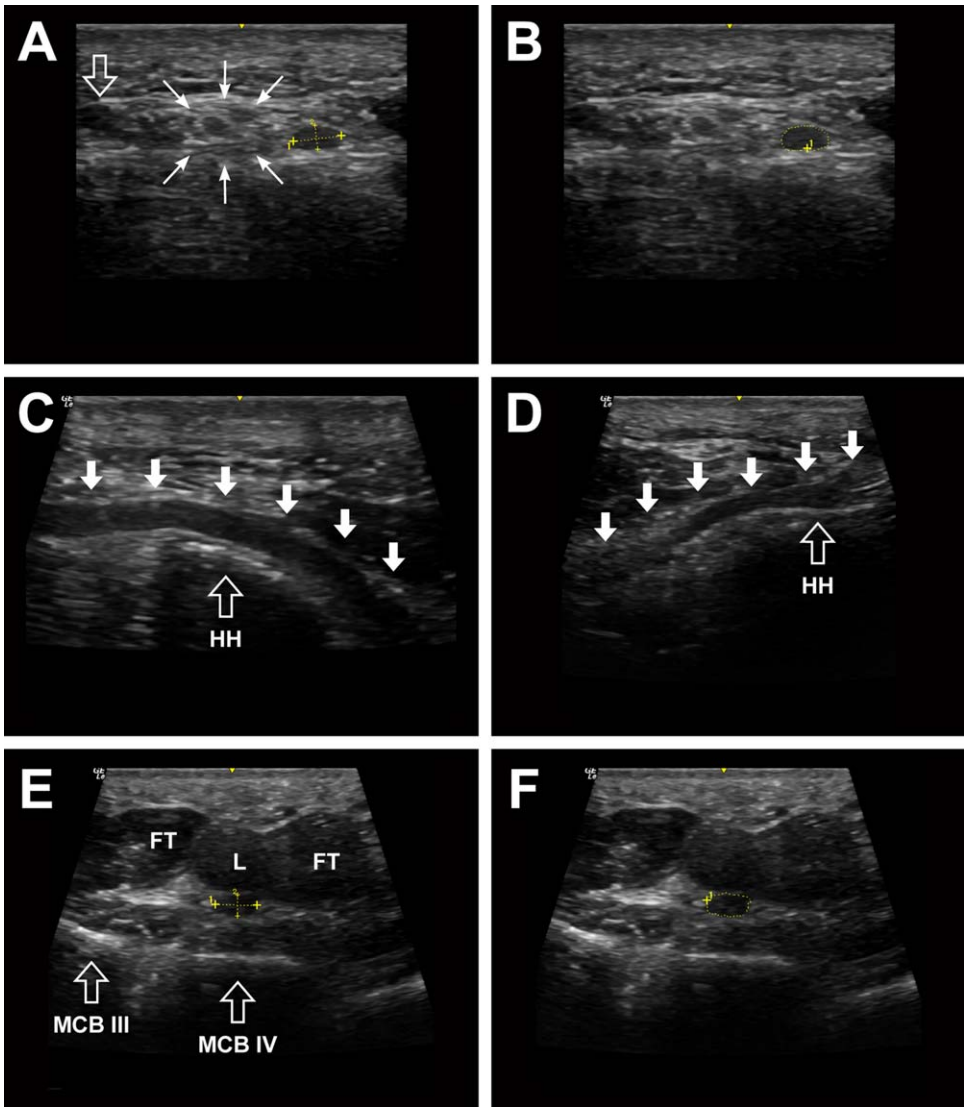


FIGURE 4. Example of ultrasound measurements directly after the separation from the ulnar nerve (**A,B**; open arrow, ulnar artery; solid arrows, superficial branch of the ulnar nerve) and atop the fourth metacarpal bone (**E,F**) in healthy volunteers. (**C,D**) Longitudinal view of the deep branch of the ulnar nerve passing the hook of the hamate (arrows, deep branch of ulnar nerve). FT, flexor tendon; HH, hook of the hamate; L, lumbrical; MCB, metacarpal bone.

It should be mentioned that, at least within the Guyon canal, MRI[12,21] is also an excellent imaging modality with which to depict the DBUN and demonstrate nerve-related pathologies. Nevertheless, the value of MRI over the entire course of the DBUN has not been evaluated. The main advantages of HRUS compared with MRI are its cost-effectiveness, excellent resolution and tissue contrast, and utility for ultrasound-guided therapy. MRI, on the other hand, allows an assessment of structures (e.g., bone) that are not fully visible with HRUS and provides a larger field of view, which is sometimes necessary to identify pathologies and to plan surgery. Therefore, we think HRUS should be considered the first-line imaging method in suspected DBUN lesions, and, if findings are positive, MRI may then be the modality of choice for further evaluation.

Ultrasound quantification of nerve size, such as nerve diameter or CSA, plays a crucial role in evaluation of entrapment neuropathies.[25] In an entrapment, regardless of whether it is idiopathic or secondary, the nerve may be focally thickened (in most cases) proximal to the lesion site.[25,26] Two locations along the course of the DBUN present a narrow space for the nerve and, thus, a possible entrapment site: a fibro-osseous tunnel formed by the tendinous origin of the hypothenar muscles (roof) and the pisohamate ligament (floor) between the pisiform and hamate bone[18] and between the tendinous arch connecting the transverse and oblique heads of the adductor

pollicis muscle at the level of the third metacarpal bone.[19]

Except for a study in which Meng *et al.*[27] measured the CSA of the DBUN distal to the bifurcation from the ulnar nerve main trunk *ex vivo*, quantitative assessment with HRUS has not yet been demonstrated. Our *in vivo* results (1.8 mm^2) are comparable to those of the aforementioned study (1.8–2.2 mm^2). Furthermore, our ultrasound measurements of the long axis diameter are in agreement with previous anatomical studies. In our study, the LD was 1.6 ± 0.3 mm and 1.5 ± 0.2 mm, whereas Schenk *et al.*[28] described 1.6 ± 0.4 mm, and Wang and Zhu[29] reported 2.1 ± 0.4 mm. To address the question of whether these measurements are reliable for depiction of DBUN lesions, additional studies are required. With the exception of two of our participants (left side of volunteers 1 and 7), our results indicate that the nerve diameter does not extensively change along its course. This may be advantageous in depiction of DBUN neuropathies if a swelling or narrowing of the nerve is present. In the aforementioned cases, the shape of the nerve did not change over its course, so cross-sectional area measurement would not provide more information. Intraindividual comparison between both wrists seems to be valuable for R1, whereas for R2 this small study population showed large differences (±0.6 mm) and additional evaluation is required. In our opinion, the data presented are reliable measurements and may serve as a reference for further, more detailed ultrasound characterization of the DBUN. Moreover, anatomical variants, such as a neural loop of the DBUN (aberrant branch of the DBUN arising proximal to the hook of the hamate and rejoining the nerve distally deep in the palm),[30] which was not detected in this study but has been reported in as many as 9% of cases,[30] should be addressed in future HRUS studies because of the possible atypical clinical presentation and danger from iatrogenic injury.

This study has several strengths and limitations. Its strengths include the use of HRUS for specific assessment of the DBUN along its entire course and confirmation of the findings by the gold standard of anatomical dissection. The limitations include the fact that *in vivo* findings were uncontrolled. However, reliability in anatomical specimens was 100%, and the DBUN in volunteers was followed into the adductor pollicis muscle. In addition, color Doppler was used in all subjects to avoid confusion with vessels. An additional limitation is that only 1 rater performed the nerve measurements, and, therefore, a definitive statement about the diagnostic reliability of DBUN measurements may be limited.

This study confirms the ability to reliably visualize the DBUN over its entire course with HRUS in anatomical specimens and healthy volunteers, and we encourage its use. Additional studies are required to assess the value of HRUS in diagnosing DBUN lesions.

The authors thank Mary McAllister for her comments on the manuscript and Aron Cserveny for his help on graphical illustrations.

Ethical Publication Statement: We confirm that we have read the Journal's position on issues involved in ethical publication and affirm that this report is consistent with those guidelines.

REFERENCES

1. Mazurek MT, Shin AY. Upper extremity peripheral nerve anatomy: current concepts and applications. Clin Orthop Relat Res 2001; (383):7–20.
2. Blair WF, Percival KJ, Morecraft R. Distribution pattern of the deep branch of the ulnar nerve in the hypothenar eminence. Clin Orthop Relat Res 1988;(229):294–301.
3. Hoogvliet P, Coert JH, Friden J, Huisstede BM, European HANDGUIDE Group. How to treat Guyon's canal syndrome? Results from the European HANDGUIDE study: a multidisciplinary treatment guideline. British J Sports Med 2013;47(17):1063–1070.
4. Assmus H, Hamer J. [Distal ulnar nerve compression at the wrist. "Loge de Guyon" and "deep ulnar branch" syndrome (author's transl.)]. Neurochirurgia (Stuttg) 1977;20(5):139–144.
5. Wang B, Zhao Y, Lu A, Chen C. Ulnar nerve deep branch compression by a ganglion: a review of nine cases. Injury 2014;45(7):1126–1130.
6. Murata K, Shih JT, Tsai TM. Causes of ulnar tunnel syndrome: a retrospective study of 31 subjects. J Hand Surg 2003;28(4):647–651.
7. Spinner RJ, Wang H, Howe BM, Colbert SH, Amrami KK. Deep ulnar intraneural ganglia in the palm. Acta Neurochir 2012;154(10):1755–1763.
8. Akuthota V, Plastaras C, Lindberg K, Tobey J, Press J, Garvan C. The effect of long-distance bicycling on ulnar and median nerves: an electrophysiologic evaluation of cyclist palsy. The Am J Sports Med 2005; 33(8):1224–1230.
9. Capitani D, Beer S. Handlebar palsy—a compression syndrome of the deep terminal (motor) branch of the ulnar nerve in biking. J Neurol 2002;249(10):1441–1445.
10. Liskutin J, Dorffner R, Resinger M, Silberbauer K, Mostbeck G. Hypothenar hammer syndrome. Eur Radiol 2000;10(3):542.
11. Harvie P, Patel N, Ostlere SJ. Prevalence and epidemiological variation of anomalous muscles at Guyon's canal. J Hand Surg 2004; 29(1):26–29.
12. Pierre-Jerome C, Moncayo V, Terk MR. The Guyon's canal in perspective: 3-T MRI assessment of the normal anatomy, the anatomical variations and the Guyon's canal syndrome. Surg Radiol Anat 2011; 33(10):897–903.
13. Bui-Mansfield LT, Williamson M, Wheeler DT, Johnstone F. Guyon's canal lipoma causing ulnar neuropathy. Am J Roentgenol 2002; 178(6):1458.
14. Caroli A, Cristiani G, Squarzina PB, De Benedittis A. [Compression of the deep palmar branch of the ulnar nerve caused by an isolated neurofibroma. Presentation of a case]. La Chir Organi Mov 1987; 72(4):381–384.
15. Vance RM, Gelberman RH. Acute ulnar neuropathy with fractures at the wrist. J Bone Joint Surg Am 1978;60(7):962–965.
16. Warhold LG, Ruth RM. Complications of wrist arthroscopy and how to prevent them. Hand Clin 1995;11(1):81–89.
17. Kiylioglu N, Akyildiz UO, Ozkul A, Akyol A. Carpal tunnel syndrome and ulnar neuropathy at the wrist: comorbid disease or not? J Clin Neurophysiol 2011;28(5):520–523.
18. Uriburu IJ, Morchio FJ, Marin JC. Compression syndrome of the deep motor branch of the ulnar nerve. (Piso-Hamate Hiatus syndrome). J Bone Joint Surg Am 1976;58(1):145–147.
19. Ruder JR, Wood VE. Ulnar nerve compression at the arch of origin of the adductor pollicis muscle. J Hand Surg 1993;18(5):893–895.
20. Seror P. Electrophysiological pattern of 53 cases of ulnar nerve lesion at the wrist. Neurophysiol Clin 2013;43(2):95–103.
21. Jacobson JA, Fessell DP, Lobo Lda G, Yang LJ. Entrapment neuropathies I: upper limb (carpal tunnel excluded). Semin Musculoskelet Radiol 2010;14(5):473–486.
22. Cowdery SR, Preston DC, Herrmann DN, Logigian EL. Electrodiagnosis of ulnar neuropathy at the wrist: conduction block versus traditional tests. Neurology 2002;59(3):420–427.

23. Zeidenberg J, Aronowitz JG, Landy DC, Owens PW, Jose J. Ultrasound-guided aspiration of wrist ganglions: a follow-up survey of patient satisfaction and outcomes. Acta Radiol 2015.
24. Davidson J, Jayaraman S. Guided interventions in musculoskeletal ultrasound: what's the evidence? Clin Radiol 2011;66(2): 140–152.
25. Cartwright MS, Walker FO. Neuromuscular ultrasound in common entrapment neuropathies. Muscle Nerve 2013;48(5):696–704.
26. Martinoli C, Bianchi S, Gandolfo N, Valle M, Simonetti S, Derchi LE. US of nerve entrapments in osteofibrous tunnels of the upper and lower limbs. Radiographics 2000;20 (Spec No):S199–S213; discussion S213–S217.
27. Meng S, Tinhofer I, Grisold W, Weninger WJ. Ultrasound-guided perineural injection at Guyon's tunnel: an anatomic feasibility study. Ultrasound Med Biol 2015;41(8):2119–2124.
28. Schenck TL, Stewart J, Lin S, Aichler M, Machens HG, Giunta RE. Anatomical and histomorphometric observations on the transfer of the anterior interosseous nerve to the deep branch of the ulnar nerve. J Hand Surg Eur 2015;40(6):591–596.
29. Wang Y, Zhu S. Transfer of a branch of the anterior interosseus nerve to the motor branch of the median nerve and ulnar nerve. Chin Med J 1997;110(3):216–219.
30. Rogers MR, Bergfield TG, Aulicino PL. A neural loop of the deep motor branch of the ulnar nerve: an anatomic study. J Hand Surg 1991;16(2):269–271.